

ANL/XFD/CP-92493

**ADVANCED PHOTON SOURCE UNDULATOR BEAMLINE TESTS OF A  
CONTACT-COOLED SILICON U-SHAPED MONOCHROMATOR\***

W.-K. Lee, P. B. Fernandez, A. Khounsary, W. Yun, and E. Trakhtenberg  
*Experimental Facilities Division*  
*Advanced Photon Source, Argonne National Laboratory*  
*Argonne, IL 60439*

CONF-970706--

September 1997

The submitted manuscript has been created by the University of Chicago as Operator of Argonne National Laboratory ("Argonne") under Contract No. W-31-109-ENG-38 with the U.S. Department of Energy. The U.S. Government retains for itself, and others acting on its behalf, a paid-up, nonexclusive, irrevocable worldwide license in said article to reproduce, prepare derivative works, distribute copies to the public, and perform publicly and display publicly, by or on behalf of the Government.

**MASTER**

DISTRIBUTION OF THIS DOCUMENT IS UNLIMITED

ph

Presented at SPIE's Annual Meeting, Conference on "High Heat Flux Engineering IV," San Diego, CA, July 27-August 1, 1997; to be published in the Proceedings.

\*This work is supported by the U.S. Department of Energy, Basic Energy Sciences-Materials Sciences, under contract #W-31-109-ENG-38.

## **DISCLAIMER**

**This report was prepared as an account of work sponsored by an agency of the United States Government. Neither the United States Government nor any agency thereof, nor any of their employees, make any warranty, express or implied, or assumes any legal liability or responsibility for the accuracy, completeness, or usefulness of any information, apparatus, product, or process disclosed, or represents that its use would not infringe privately owned rights. Reference herein to any specific commercial product, process, or service by trade name, trademark, manufacturer, or otherwise does not necessarily constitute or imply its endorsement, recommendation, or favoring by the United States Government or any agency thereof. The views and opinions of authors expressed herein do not necessarily state or reflect those of the United States Government or any agency thereof.**

**DISCLAIMER**

**Portions of this document may be illegible  
in electronic image products. Images are  
produced from the best available original  
document.**

# Advanced Photon Source undulator beamline tests of a contact-cooled silicon u-shaped monochromator

W-K Lee, P. B. Fernandez, A. Khounsary, W. Yun and E. Trakhtenberg  
Advanced Photon Source  
Argonne National Laboratory  
9700 S. Cass Avenue  
Argonne, IL 60649.

## Abstract

At the Advanced Photon Source (APS), undulator insertion devices are capable of producing x-ray beams with a total power of about 5 kW and normal incidence heat fluxes of about  $170 \text{ W/mm}^2$  at 30 m from the source. On beamlines in which the first optical element is a mirror, the reflected beam from the mirror still carries considerable power and power density. Depending on its location, the monochromator downstream of the mirror might be subject to 300 W total power and  $5 \text{ W/mm}^2$  normal incidence heat flux. Thus, it is still necessary to carefully design a monochromator that provides acceptable performance under these heat loads. A contact-cooled u-shaped monochromator may be used in this case. The main feature of the u-shaped monochromator is that, by carefully selecting the geometry and cooling locations, it passively corrects for some of the thermally induced crystal distortions. We present experimental and computational results of a contact cooled u-shaped monochromator tested on an APS undulator beamline. The results are encouraging and compare favorably with liquid-gallium internally cooled crystals.

## 1. Introduction

At the Advanced Photon Source (APS), undulator insertion devices are capable of producing x-ray beams with total power of about 5 kW and normal incidence heat fluxes of about  $150 \text{ W/mm}^2$  at 30 m from the source. In order to preserve the beam brilliance, optical components must be able to handle these heat loads with minimal thermally induced distortions. The vertical opening angle of the undulator radiation is usually on the order of 2 to 3 arc seconds. The optical components must, therefore, be free of distortion at the arc second level. Thus, innovative cooling techniques are required for all first optical components of the beamline. For undulator beamlines in which the first optical component is a crystal monochromator, the use of diamonds [1] and cryogenically cooled silicon [2] has been successfully implemented. In the case where the first optical element is a mirror [3], an innovative contact cooling technique is being used [4].

On beamlines in which the first optical element is a mirror, the reflected beam (usually referred to as a "pink" beam) still carries considerable power and power density. For example, for the APS sector-2 undulator beamline, the crystal monochromator downstream of the first mirror can be subjected to a maximum of 300 W total power and  $5 \text{ W/mm}^2$  surface power density [5]. Thus, although the mirror bears the brunt of the heat load, thermal management of the downstream monochromator is still necessary. A contact-cooled monochromator, in the shape of the letter U, has been designed for this purpose (Figure 1). The main feature of the u-shaped monochromator is that, by carefully selecting its geometry and cooling locations, it passively corrects some of the thermally induced

crystal distortions [6]. The simplicity, ease of fabrication and mounting, low risk of vacuum breach, and much lower cost compared with direct (internally) cooled crystals make the u-monochromator a very attractive option in this thermal load range. In this paper, we present computer simulations and experimental results from measurements taken at the APS. The measurements were performed at sector-1, where the first optical component is the monochromator, even though the u-monochromator is designed for use in a beamline where the first optical element is a mirror.

## **2. Experimental Setup**

The dimensions of the u-monochromator tested are shown in Figure 1a. The diffraction surface is (1-1-1). It was fabricated from an ingot of single-crystal float-zone silicon (purchased from Topsil, Inc.). The crystal was thoroughly etched after machining. Thermal contact with a cooled nickel-plated copper block was made via a 25%-75% indium-gallium eutectic (see Figure 1b). As usual, the liquid metal was rubbed onto the surfaces with a cotton swab to ensure wetting. The crystal is thus held on the bottom and the sides via surface tension. Two adjustable end blocks were used to ensure that the crystal does not move within the cooled copper block. Room temperature water was used to cool the copper block. The flow rate was about 0.75 gpm.

The mounted crystal was installed in the 1-ID Kohzu-Seiki double-crystal monochromator (DCM). The "second crystal" of the DCM was also silicon (1-1-1), and it has a fine piezoelectric transducer (PZT) rotation adjustment. The experimental setup is shown in Figure 2. Slits upstream of the monochromator determined the size of the white beam on the crystal. A video camera monitored the fluorescence from the crystal, and an infrared (IR) camera monitored the crystal surface temperature. By looking at the images from the two cameras, the vertical white beam slits were set so that the white beam totally covered the crystal diffraction surface in the beam direction. For best performance, it is desirable to have the white beam cover the entire crystal surface in the tangential direction [6] so that there are no steep power gradients on the crystal surface in the tangential direction. The size of the white beam (normal incidence) was about 2.2 mm vertical by 3 mm horizontal.

Several windows and window-protection filters (a total of 500  $\mu\text{m}$  of graphite, 170  $\mu\text{m}$  of diamond and 750  $\mu\text{m}$  of Be) are between the source and the crystal. These absorb about 20% of the total power from the insertion device. Due to a misalignment of the white-beam slits horizontally, only half the actual x-ray beam was incident on the crystal. That is, the horizontal incident power profile of the beam was actually half a parabola. The vertical and horizontal power profiles of the undulator beam incident on the u-monochromator are shown in Figures 3 and 4, respectively. The misalignment was due to the particle beam not being in the optimum orbit. (Instead of trying to have the orbit moved to the optimum position and risk losing the beam altogether, we decided to continue with the measurements.)

The measurements were performed at  $\theta = 6.3^\circ$  (18 keV for Si (1-1-1)). This angle (energy) was chosen so that with a relatively open undulator gap ( $\sim 25$  mm), the surface power density would be about  $3 \text{ W/mm}^2$ . This way, by adjusting the undulator gap (thereby changing the heat load), we could obtain data in the  $0.5$  to  $5 \text{ W/mm}^2$  range. Rocking curves were obtained by tweaking the second crystal PZT. Two types of data were taken; one with wide open downstream monochromatic slits and the other with very small ( $0.2 \text{ mm} \times 0.2 \text{ mm}$ ) movable monochromatic slits. The latter measurement allowed us to map out the tangential slope errors on the u-monochromator by only looking at the part of the monochromatic beam that comes from a particular spot on the u-monochromator. The relative positions of the rocking curve peaks, together with the

positions of the monochromatic slits provide information on the surface tangential slope errors. Calorimetry was used to directly measure the amount of power incident on the crystal. Data were taken at four different undulator gaps starting at 40 mm. The storage ring current was between 80 and 100 mA for all of the data presented here.

#### Low-power data

At 40 mm undulator gap, the heat load on the crystal was minimal, and the goal of this "cold beam" measurement was to determine if the crystal had any mounting-induced strains. The measured full beam rocking curve (see Figure 5) was 4.3 arc seconds (FWHM), as predicted by theory. Using the monochromatic slits, five different points on the crystal surface were mapped for their tangential slope errors. The rocking curve peak positions for these points were all within 0.5 arc seconds (instrumental resolution) of one another, indicating that the crystal was indeed unstrained.

#### High-power data

Figure 6 shows rocking curve scans at five different vertical monochromatic slit locations (i.e., looking at the beam reflected from different spots on the u-monochromator) for the case in which the undulator gap was 25 mm. The sampled spots were taken tangentially (along the beam direction) through the center of the crystal. The measured power on the crystal was about 66 W. The surface peak heat flux was estimated to be about  $2.6 \text{ W/mm}^2$  ( $\pm 10\%$ ). The envelope of all the peaks is a measure of the overall tangential slope error on the crystal surface. Figure 7 shows the rocking-curve peak positions as a function of the position along the crystal in the beam direction. This can also be interpreted as a map of the tangential slope error (arbitrary zero) of the crystal. It is seen that the relative peak positions vary linearly with the position of the sampled spot on the crystal surface. This, together with information regarding the sense of the PZT rotations, shows that the surface of the u-monochromator is convex with a parabolic shape. A simple linear fit to the peak positions shows that the slope error is about 0.2 arc seconds per mm length of the u-monochromator along the beam direction. From the IR camera, the maximum temperature on the crystal was about  $50^\circ\text{C}$ , and the maximum temperature difference on the crystal surface was  $14^\circ\text{C}$ . The maximum temperature difference on the crystal surface is the difference between the hottest part of the crystal (center of the white beam) and the part of the crystal where there was no beam, which, in this case, was just to the side (transverse direction) of the crystal.

Figure 8 shows the rocking-curve peak positions (arbitrary zero) as a function of the position along the crystal in the beam direction for the case in which the undulator gap was 23 mm. The measured power on the crystal was about 100 W, and the surface power density was estimated to be about  $3.5 \text{ W/mm}^2$  ( $\pm 10\%$ ). A linear fit to the peak positions indicate that the slope error is about 0.4 arc seconds per mm length of the u-monochromator along the beam direction. The maximum temperature on the crystal was about  $71^\circ\text{C}$ , and the maximum temperature difference was about  $21^\circ\text{C}$ .

### 3. Computer Simulations

In order to compare the experimental results with the analytical results, the tested monochromator was analyzed using an approximation to the indicated heat load for the case of the 25-mm-gap undulator x-ray beam. Using a linear approximation to the incident vertical and horizontal heat flux profiles, a surface heat flux distribution of the form

$$F(v,h) = 2.6 (0.5 + h/3) (1 - 0.05 v)$$

is assumed, where  $v$  and  $h$  refer to vertical (tangential) and horizontal (sagittal) axes. The origin is taken to be at the center of the reflecting surface. Because of symmetry, one half of the 20-mm-long monochromator was modelled. The range of  $v$  and  $h$  are (0 to 10) and (-1.5 to 1.5) in units of mm, respectively. The total incident beam power, obtained by integrating the above equation (and multiplying by 2) is about 60 W, consistent with measurements.

The bottom face and 13 mm height on both sides of the monochromator are cooled (Figure 1). A contact conductance of  $30000 \text{ W/m}^2\text{-K}$  for the monochromator cooling block interface with In/Ga interstitial filler and constant material properties (thermal expansion coefficient and thermal conductivity) of silicon are assumed. Assuming a coolant temperature of  $30^\circ\text{C}$ , the maximum and minimum temperatures on the reflecting surface are about  $52$  and  $36^\circ\text{C}$ , respectively. The temperature difference of  $16^\circ\text{C}$  compares favorably with the measured  $14^\circ\text{C}$  value. The overall minimum temperature in the crystal is  $31^\circ\text{C}$  at the cooling-block interface.

Assuming a uniform thermal contact between the monochromator and the cooling block, calculations show that about one half of the heat is removed through the bottom and the other half through the walls of the monochromator. Because of beam profile asymmetry in the horizontal direction, the wall adjacent to the peak heat flux conducts out slightly more than a quarter of the heat load.

The maximum equivalent stress calculated is about  $5.5 \text{ MPa}$  ( $800 \text{ psi}$ ). The tangential slopes are computed along the center of the reflecting surface and along lines parallel to it. These have nearly identical profiles. The tangential slope along the center line is plotted in Figure 9. As shown, the maximum slope error in the interval  $\pm 8 \text{ mm}$  of the monochromator is  $\pm 2$  arc seconds. Figure 9 also shows close agreement between calculations and measurements.

The calculated sagittal slope is about  $\pm 5$  arc seconds across the beam footprint. This sagittal slope error is comparable to the horizontal particle beam divergence at the APS (FWHM particle beam horizontal divergence is about  $12$  arc seconds). While this sagittal error has minimal effect on the vertical divergence of the beam, it does increase its horizontal divergence.

Finally, in order to show the advantage of the u-shaped monochromator, the expected performance for a block shaped (or flat) monochromator (with the reflecting surface brought up to the level of the wings) is determined. The expected slope error plotted in Figure 9 indicates a 50% deterioration from the u-shaped monochromator. Identical cooling is assumed in both cases.

#### 4. Discussion and Conclusion

It is useful to compare the performance of the u-monochromator with other monochromators. Because the heat load varies tremendously between synchrotron facilities and between different beamlines, it is usually not possible for direct performance comparisons. In this case, fortunately, we have data from previous measurements under

very similar heat load conditions, i.e.,  $\sim 3 \text{ W/mm}^2$  surface power density and  $\sim 70 \text{ W}$  total power, for an internally liquid-gallium-cooled slotted crystal. For this comparison, we ignore the differences in the white beam spectrum for the various cases. Assuming that the thermally induced strains add in quadrature to the "cold" crystal, Table 1 compares the measured performance of a liquid-gallium-cooled slotted crystal [7] with the present contact-cooled u-monochromator. It is shown that the performance of the water-contact-cooled u-monochromator is comparable to a liquid-gallium direct-cooled slotted crystal! It is interesting to note that the maximum temperature difference (defined as the difference between the maximum temperature and the temperature where there is no beam) for the case of the u-monochromator is about twice that of the liquid-gallium-cooled monochromator. Normally, one would expect that the higher temperature difference would result in higher slope errors. But in this case, by design, the crystal corrects for the slope error, and therefore, the actual slope errors are reduced.

In considering Figures 7, 8 and Table 1, it is important to note the following. In most cases, only the central cone of the undulator radiation is utilized. Because the FWHM normal incidence vertical size of the central-cone at distances of 60 m is about 1 mm, the relevant slope errors, across the u-monochromator, are substantially less than the overall slope errors listed in Table 1. That is, at 18 keV, the central cone beam footprint is about  $1 \text{ mm} / \sin(6.3^\circ) = 9.1 \text{ mm}$ . Thus, the relevant slope error is about  $0.4 \text{ arc sec/mm} \times 9.1 \text{ mm} = 3.6 \text{ arc seconds}$ . This is compared to the value of 8.5 arc seconds as stated in Table 1.

Table 1: Performance comparison between the u-monochromator and a direct liquid-gallium-cooled slotted monochromator, tested at CHESS and the APS. The measured values of the thermally induced slope errors are stated over the entire beam footprint.

	Total power (watts)	Surface power density ( $\text{W/mm}^2$ )	Thermally induced slope error (arc seconds)	Beam footprint (mm)	Maximum temperature difference ( $^\circ\text{C}$ )
u-mono @ APS (25 mm gap)	66	2.6	7.5	20	14
u-mono @ APS (23 mm gap)	100	3.5	8.5	20	21
slotted liq.-Ga-cooled mono @ CHESS	80	4	7.4	12	10
slotted liq.-Ga-cooled mono @ APS	60	2	5.2	10	2.2

In conclusion, we have demonstrated that the u-monochromator does indeed perform quite well and that, in this heat load range, its performance is comparable to directly cooled



(room temperature) silicon crystals. The advantages of the u-monochromator over that of internally cooled crystals are many. Most directly cooled crystals require silicon-silicon or silicon-metal bonding and a silicon-metal leak-proof joint. Previous experience shows that such fabrication and/or mounting procedures usually result in strains of about 1 to 10 arc seconds in the silicon crystal (eg., see ref [8]). We have shown that, for the u-monochromator, due to the simplicity of the crystal design and the absence of direct cooling, there were no residual strains in the mounted crystal. Furthermore, no silicon-metal joints are needed, and the risk of a vacuum breach is greatly reduced. The cost of the monochromator is also greatly reduced. Compared to the cost of a slotted or patterned direct (internally) cooled crystals (~\$20 K) and a liquid gallium pump (~\$100 K), the cost of the u-monochromator system is negligible (~\$2 K).

## 5. Acknowledgements

We wish to thank M. Keefe, F. Krasnicki, S. Xu, and R. Dejus for their assistance. This work is supported in part by the U. S. Department of Energy, BES Materials Sciences under Contract No. W-31-109-ENG-38.

### Figure Captions:

Figure 1: (a) Dimensions of the u-monochromator tested. (b) Diagram of the u-monochromator sitting in the nickel-plated cooled copper mount. Thermal contact was achieved via the use of an indium-gallium eutectic interface. For the crystal tested here, the dimensions are as follows:  $w_1 = 6$  mm,  $h_2 = 10$  mm,  $h_3 = 7$  mm,  $w_0 = 20$  mm,  $h_0 = 17$  mm, and  $h_1 = 13$  mm.

Figure 2: The experimental setup at the APS SRI-CAT Sector 1-ID beamline.

Figure 3: Vertical normal incidence heat flux (through the hottest part of the beam) onto the crystal for the case with a 25 mm undulator gap. The solid line is the true beam profile, while the dotted line is the linearized beam profile used in the finite element analysis, as described in section 3.

Figure 4: Horizontal normal incidence heat flux (through the hottest part of the beam) onto the crystal for the case with a 25 mm undulator gap. The solid line is the true beam profile, while the dotted line is the linearized beam profile used in the finite element analysis (FEA), as described in section 3.

Figure 5: Full ("cold") beam rocking curve at 40 mm undulator gap.

Figure 6: Overplot of rocking curves taken at different vertical monochromatic slit positions. The size of the slit was 0.2 mm x 0.2 mm, and thus the size of each sampled spot on the crystal surface was about 0.2 mm H x 1.8 mm V. Each vertical monochromatic slit position corresponds directly to a spot on the crystal surface. The inlay schematic depicts a top view of the crystal, and the small black squares (■) denote the sampled area for each of the rocking curves.

Figure 7: The relative tangential slope on the crystal as a function of the tangential position on the crystal for the case of a 25 mm undulator gap. (The relative tangential slopes are simply the relative peak positions from Figure 6). The straight line is a linear fit to the data and the parameters of the fit are shown in the inlay.

Figure 8: The relative tangential slope on the crystal as a function of the tangential position on the crystal surface for the case of a 23 mm undulator gap. The straight line is a linear fit to the data, and the parameters of the fit are shown in the inlay.

Figure 9: Comparison of FEA results with actual measurements for the 25 mm undulator gap case.

### References

- [1] P. B. Fernandez, T. Graber, S. Krasnicki, W. K. Lee, D. M. Mills, C. S. Rogers, and L. Assoufid, Proceedings of the 1997 National Synchrotron Radiation Instrumentation Conference, to be published by Review of Scientific Instruments.
- [2] C. S. Rogers, D. M. Mills, W. K. Lee, P. B. Fernandez, and T. Graber, SPIE Proceedings, Volume 2855, p171 (1996).
- [3] W. Yun, B. Lai, D. Shu, A. Khounsary, Z. Cai, J. Barraza, and D. Legnini, Rev. Sci. Instrum., 67(9), CD ROM, (1996).
- [4] A. Khounsary and W. Yun, Rev. Sci. Instrum., 67(9), CD ROM, (1996).
- [5] W. Yun, A. Khounsary, B. Lai, and E. Gluskin, Argonne National Laboratory Technical Bulletin ANL/APS/TB-2, September 1992.
- [6] A. Khounsary, W. Yun, E. Trakhtenberg, S. Xu, L. Assoufid and W. K. Lee, SPIE Proceedings, Volume 2855, p. 232 (1996).
- [7] A. T. Macrander, W. K. Lee, R. K. Smither, D. M. Mills, C. S. Rogers and A. M. Khounsary, Nucl. Instrum. Meth. A319, p188 (1992), and recent commissioning tests on the 1-ID beamline.
- [8] T. Graber, S. F. Krasnicki, P. B. Fernandez, and Q. Tong, these proceedings.

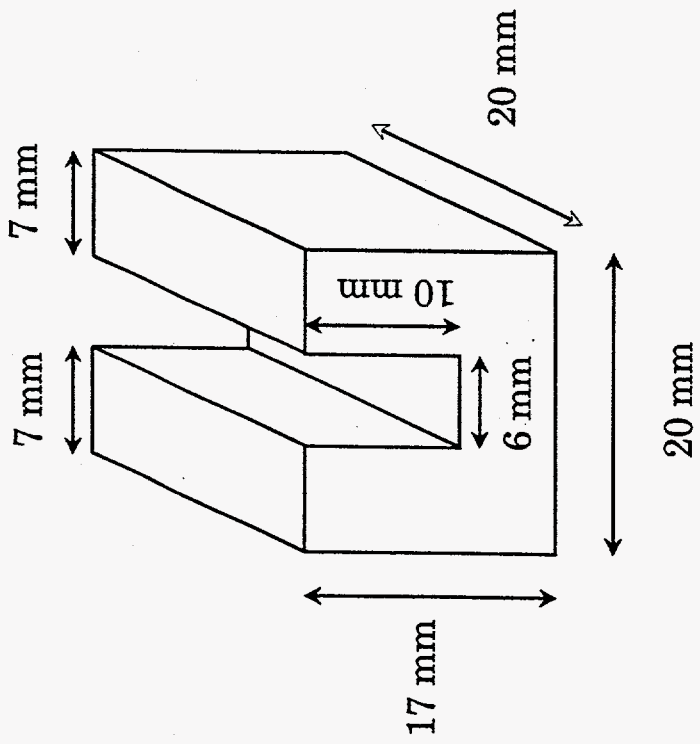
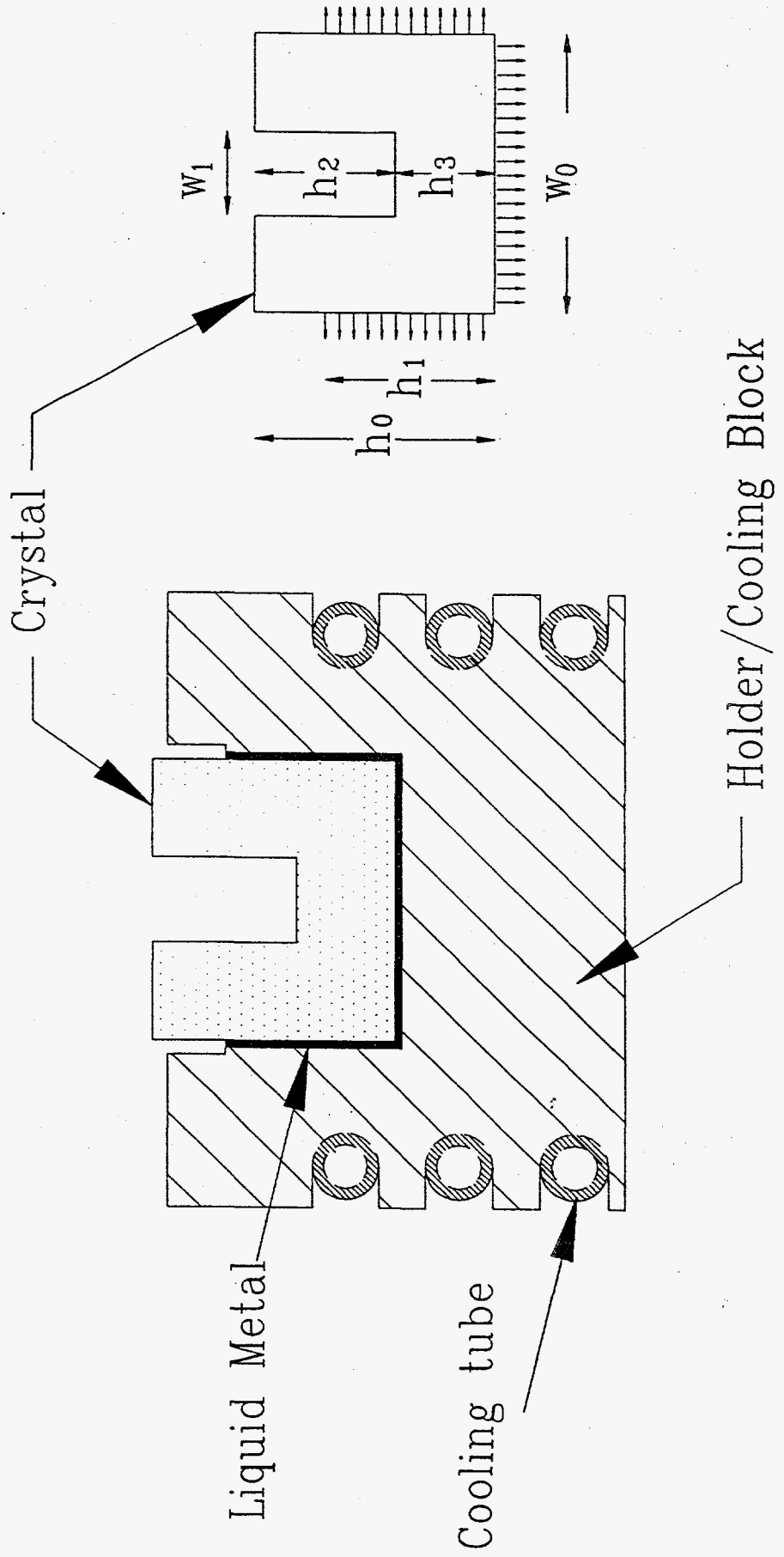


Fig 1 a

Fig 1 b



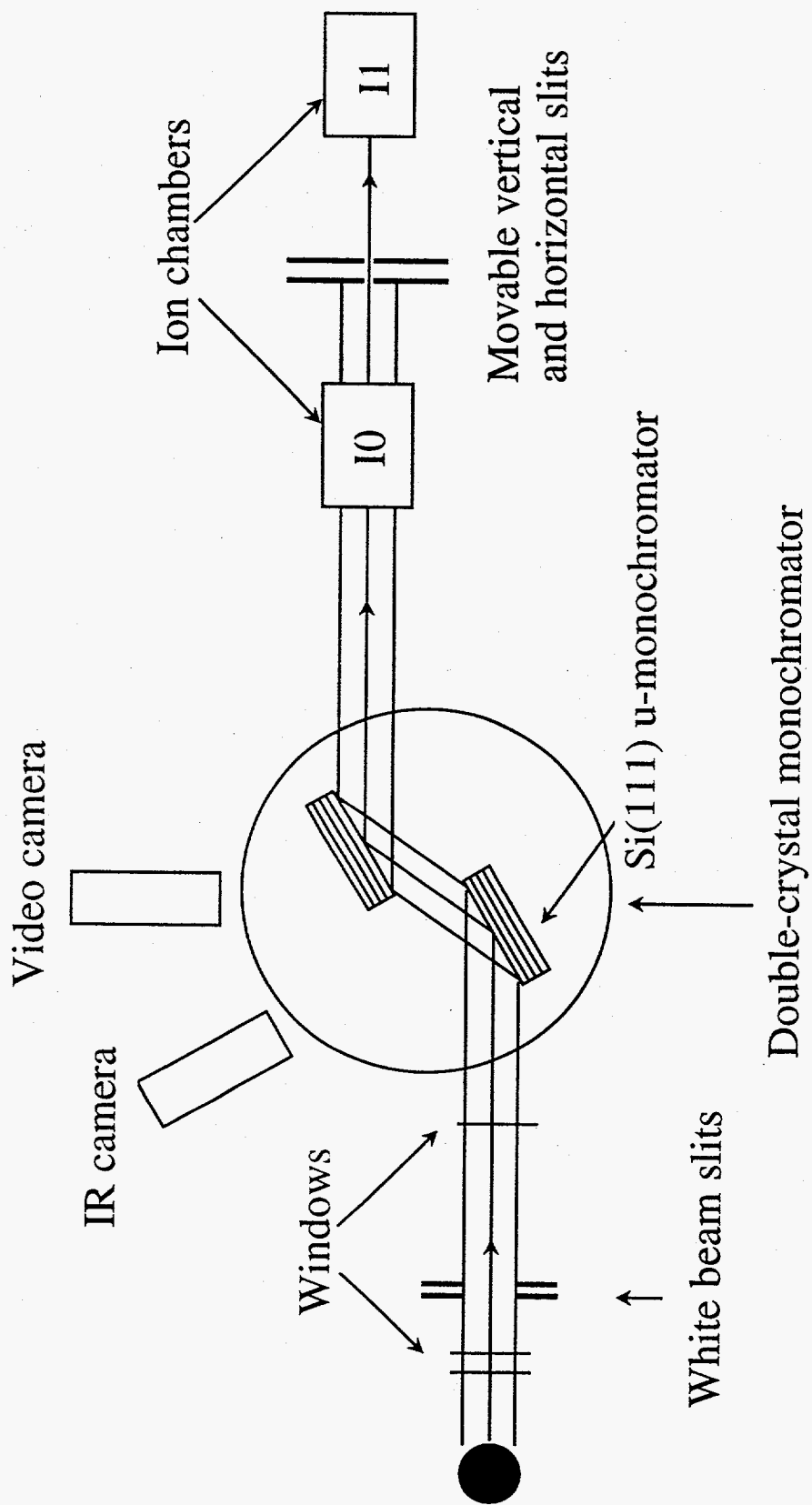


Figure 2

Figure 3

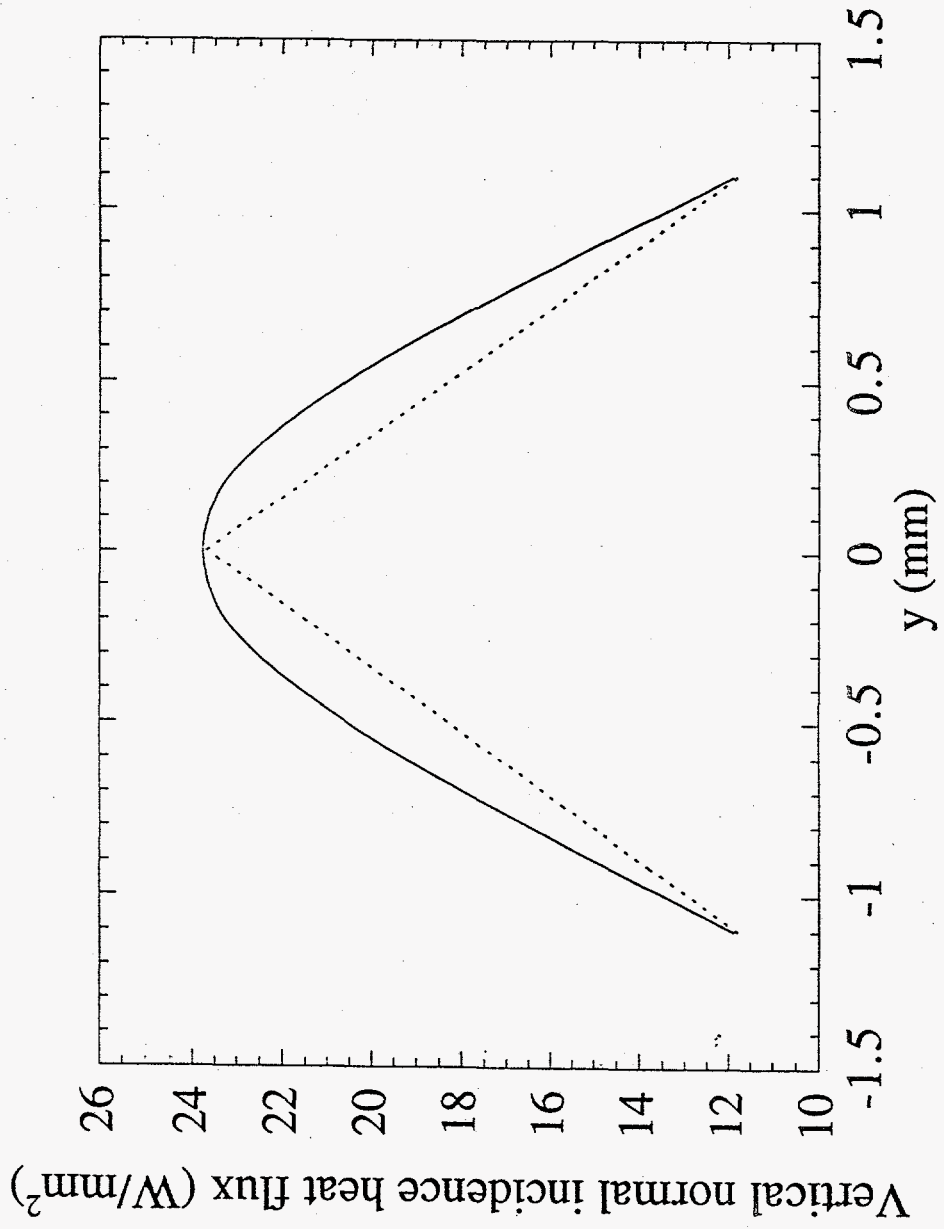


Figure 4

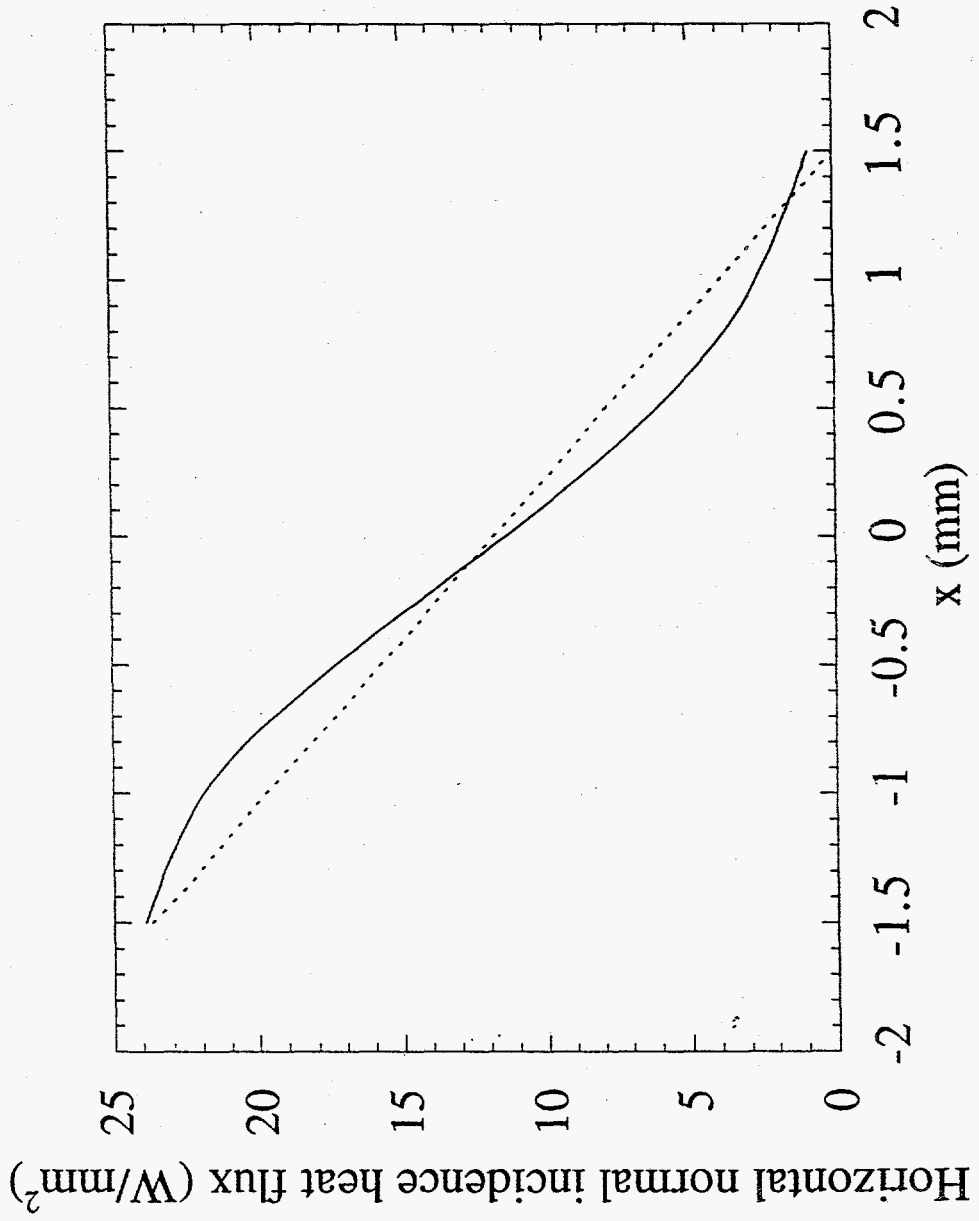


Figure 5

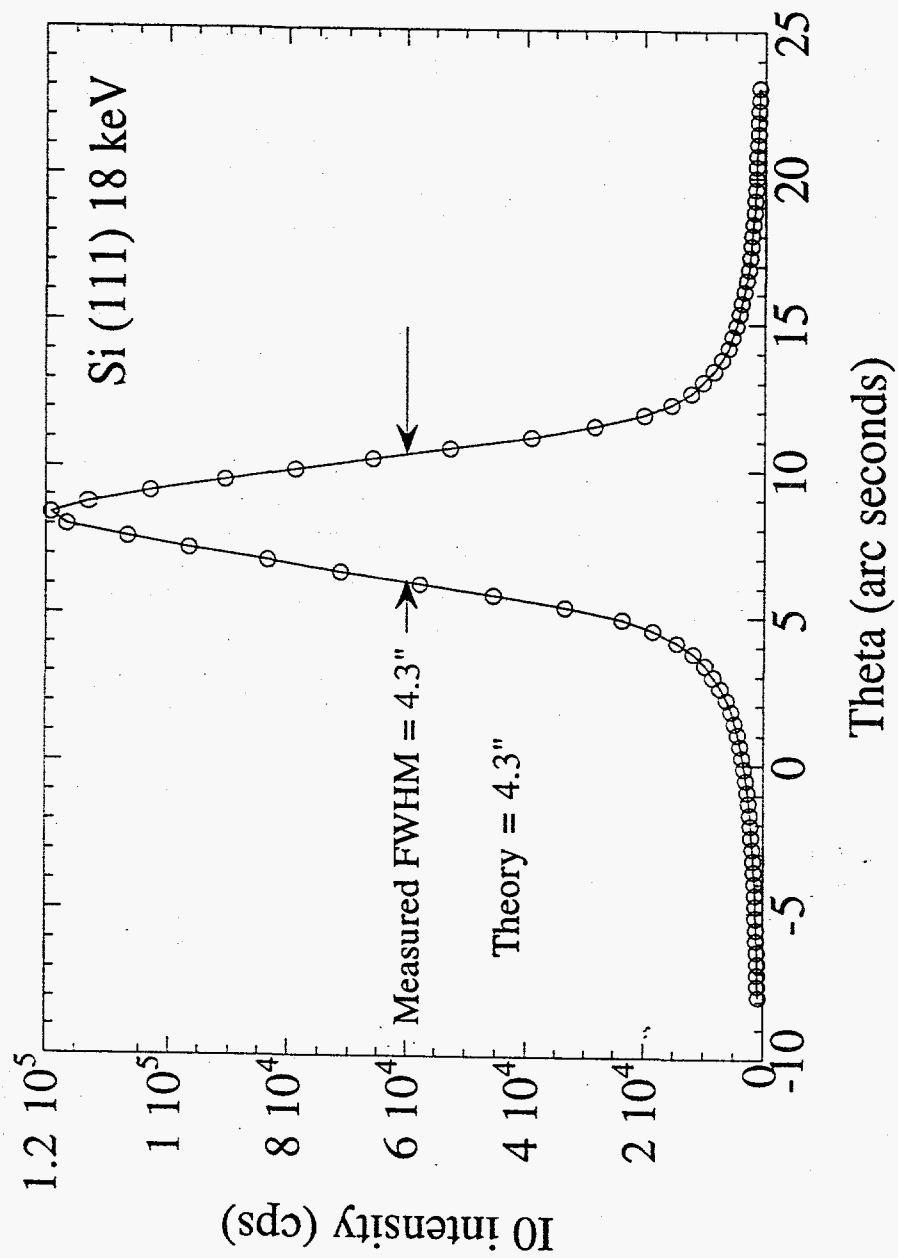




Figure 6

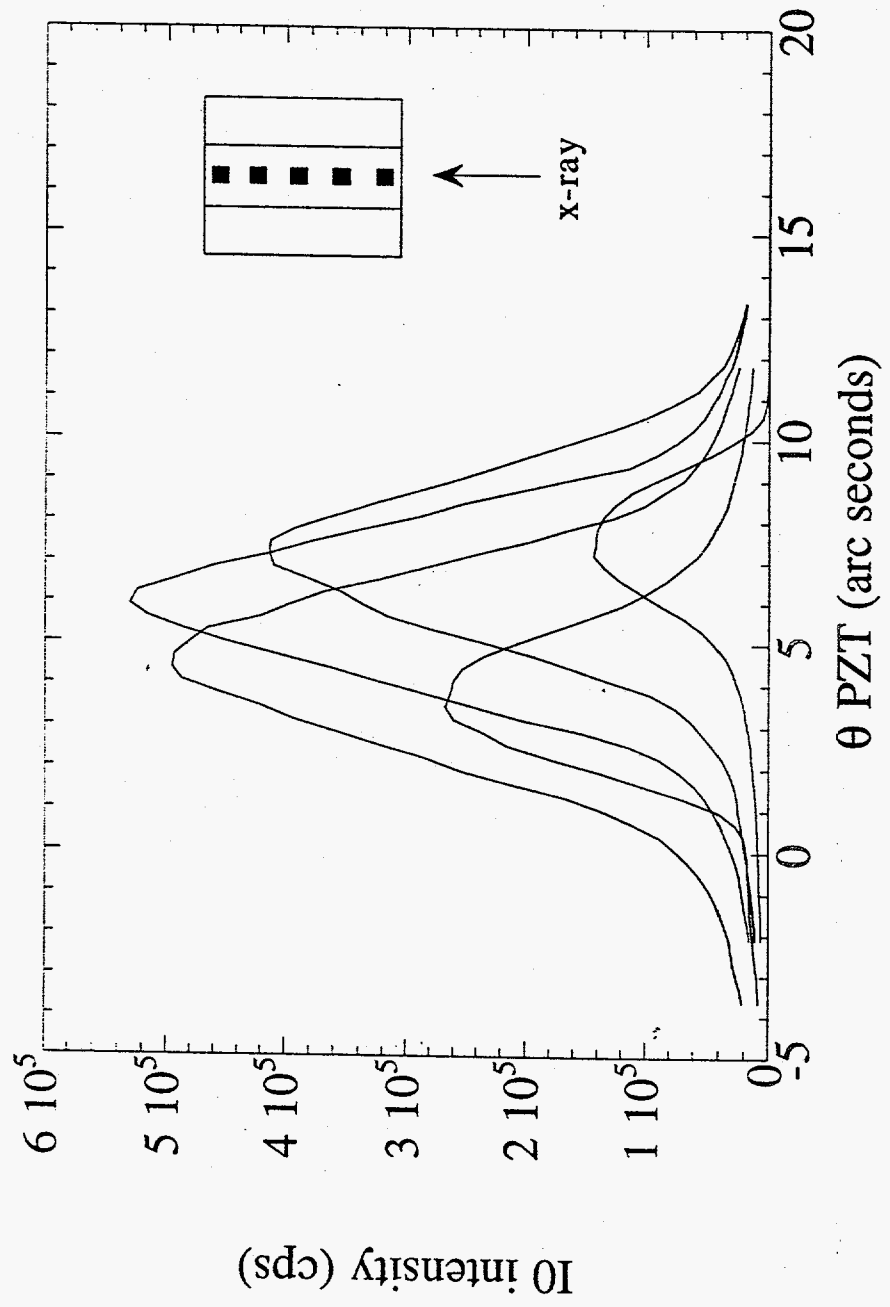


Figure 7

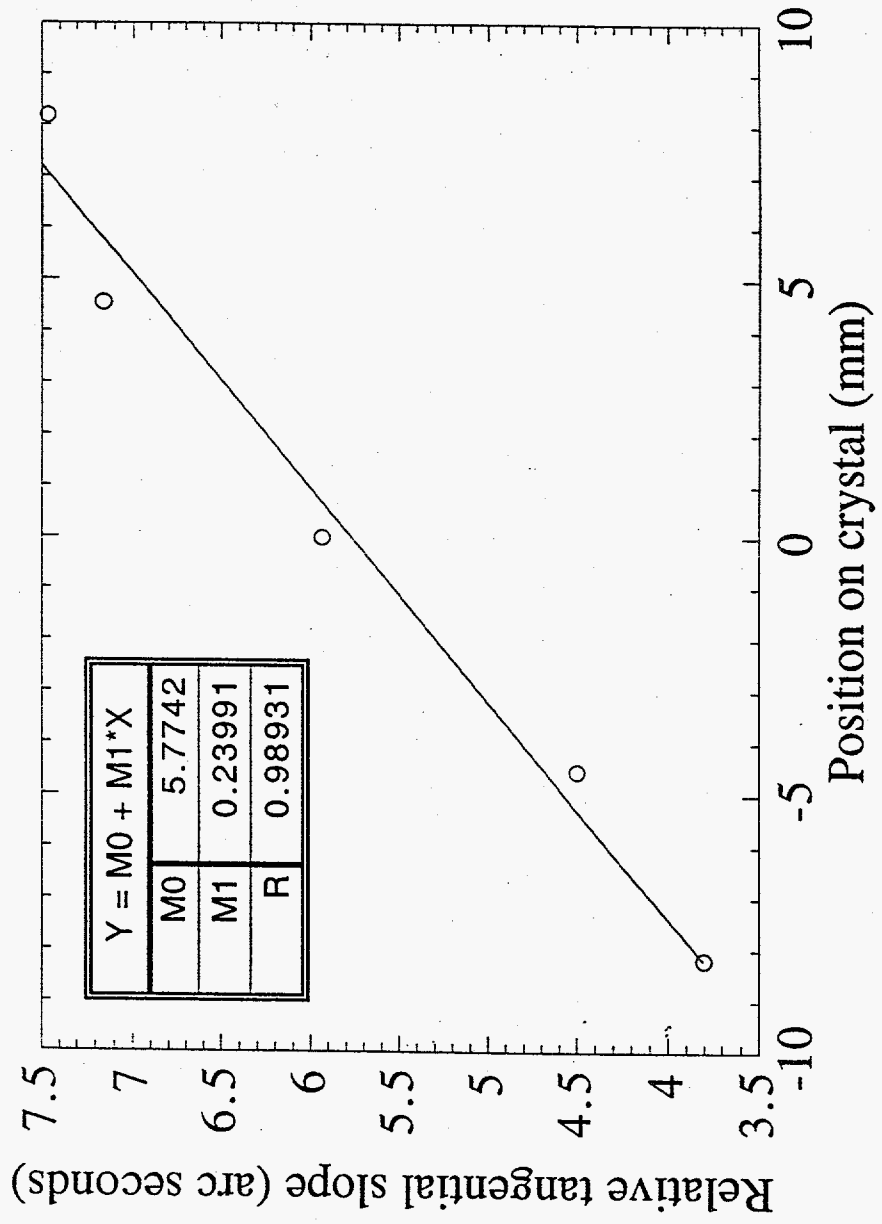


Figure 8

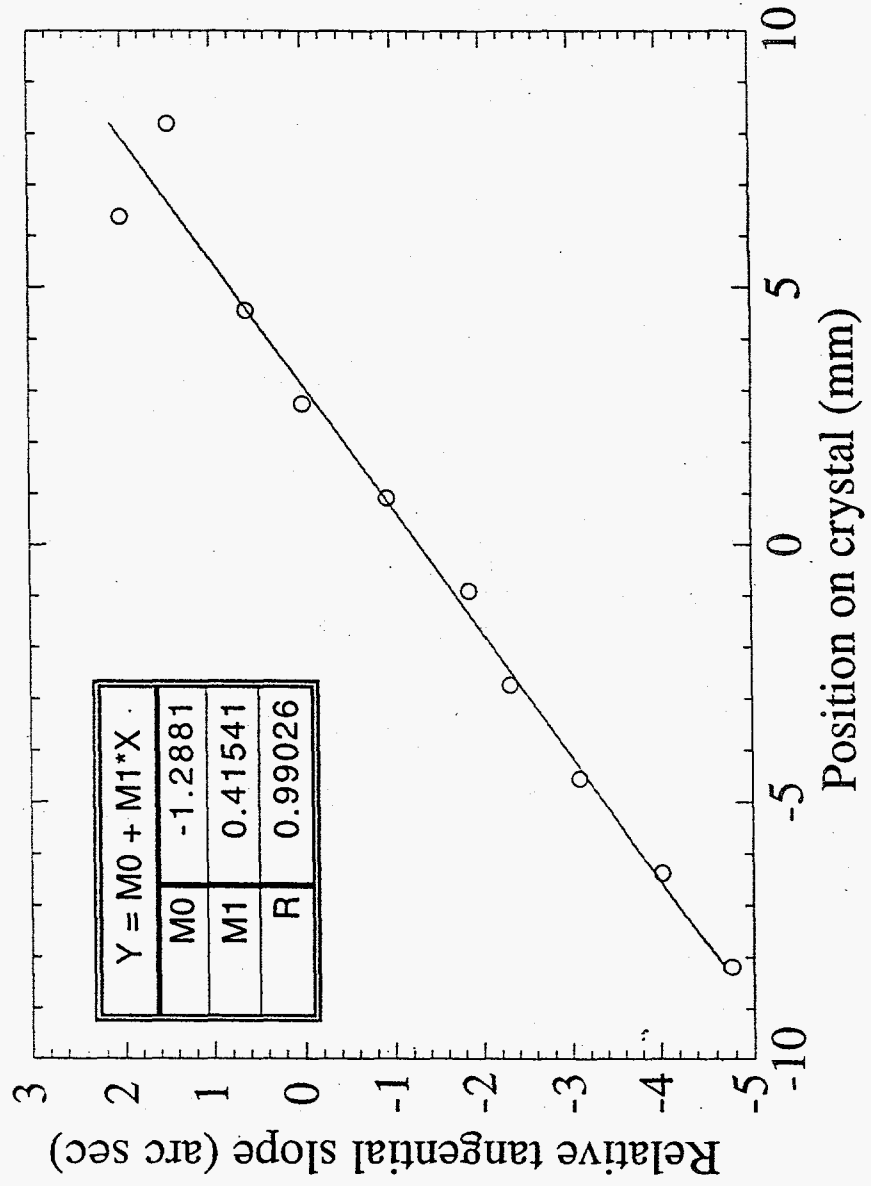


Figure 9

